



PERGAMON

Available online at www.sciencedirect.com

SCIENCE @ DIRECT®

Solid State Communications 125 (2003) 617–622

**solid
state
communications**

www.elsevier.com/locate/ssc

Excitonic field screening and bleaching in InGaN/GaN multiple quantum wells

Fei Chen*, W.D. Kirkey, M. Furis, M.C. Cheung, A.N. Cartwright

Department of Electrical Engineering, State University of New York at Buffalo, Bonner Hall 119, Buffalo, NY 14260, USA

Received 31 October 2002; accepted 6 January 2003 by J. Kuhl

Abstract

Photoinduced carrier dynamics in a sequence of InGaN/GaN multiple quantum wells (MQWs) are studied by employing steady state and ultrafast spectroscopy at room temperature. Time-resolved photoluminescence (PL) measured short carrier lifetimes of ~ 140 ps at room temperature. Steady state differential transmission was used to measure the in-well field screening due to the photoinjected carriers. The observed offset in emission energy from excitonic screening energies is consistent with the emission of carriers through localized states slightly below the excitonic resonance energy. Furthermore, time-resolved differential transmission with amplified pulses, where significant carrier densities can be optically generated, provides evidence of both excitonic bleaching and field screening in these InGaN quantum wells (QWs). The comparison of the time-resolved differential absorption spectra at various carrier densities allows us to identify different carrier recombination dynamics in the InGaN well and to separate the field screening from the bleaching effects. Finally, the extreme prolongation of the carrier recombination lifetime up to ~ 4 μ s suggests the spatial separation between electrons and holes under the large in-well fields. © 2003 Elsevier Science Ltd. All rights reserved.

PACS: 78.67.De; 78.47. + p; 71.35. – y

Keywords: A. Quantum wells; D. Optical properties; E. Time-resolved optical spectroscopies

1. Introduction

Significant research and commercial interests have continued to focus on the development of indium-based III-nitride materials and associated devices for UV-visible light emitters [1,2]. The success in developing light sources has included the commercialization of blue, green and amber light emitting diodes and violet laser diodes. In spite of these developments, the emission mechanisms of these materials are still not fully understood due to the complex material physics, including indium clustering resulting from phase separation [3,4] in InGaN alloys and strain-induced piezoelectricity [5] due to the large lattice constant mismatch between GaN and InGaN. The incorporated

InGaN/GaN quantum wells (QWs) within these structures and the resulting emission, absorption, and associated field and localization effects significantly complicate the understanding of these materials. The further development of solid-state light sources, particularly lasers, based on these materials depends upon a complete understanding of these emission mechanisms.

The direct measurement of changes in absorption resulting from photoinjected carriers using pump/probe spectroscopy has proven invaluable in unraveling field effects on absorption in [111] InGaAs/GaAs materials with piezoelectric fields in the QWs [6–8]. To date, several groups have discussed the blue shift of the photoluminescence (PL) peak energy in InGaN/GaN heterostructures with increasing carrier injection. The observed carrier dynamics has been described using models that attribute the behavior to either the reduction of the quantum-confined Stark effect due to in-well field screening [5,9,10] or through

* Corresponding author. Tel.: +1-716-6453123; fax: +1-716-6453656.

E-mail address: feichen@eng.buffalo.edu (F. Chen).

band-filling of the energy band tail states [11,12] or both [13,14]. The main reason that these studies have not been able to directly elucidate these complicated dynamics is because traditional time integrated PL and time-resolved PL measurements allow only the radiative recombination dynamics to be directly characterized. As demonstrated in piezoelectric materials, ultrafast differential transmission spectroscopy can extract the needed carrier transport and recombination dynamics by separating the field screening behavior from the band-filling effects [8]. A few differential transmission measurements on InGaN/GaN QWs that have focused on stimulated emission processes and carrier capture times have been reported [15–17]. However, of those experiments, none has spectrally and temporally resolved the resulting changes in absorption coefficient due to in-well field screening. In this article, we present steady state, time-resolved differential transmission and time-resolved PL to identify different carrier recombination dynamics in InGaN/GaN multiple quantum wells (MQWs). The contribution of the in-well screening of the piezoelectric field to the changes in the absorption coefficient is separated from, and compared to the excitonic bleaching. The estimated in-well field at the transition point between field screening and excitonic bleaching determined using this method is consistent with the theoretical value of the piezoelectric field in the strained InGaN well.

2. Sample structures

The samples in this study are two undoped InGaN/GaN MQW structures deposited by metal organic vapor phase epitaxy on a hydride vapor phase epitaxy grown GaN/Sapphire substrate. As determined by X-ray diffraction, sample 1 is an $\text{In}_{0.1}\text{Ga}_{0.9}\text{N}/\text{GaN}$ MQW which consists of six periods of 100 Å thick wells and 150 Å thick barriers, and sample 2 is an $\text{In}_{0.04}\text{Ga}_{0.96}\text{N}/\text{GaN}$ MQW which has six periods of 100 Å thick wells and 110 Å thick barriers. The pseudomorphically strained InGaN layer grown on top of a GaN buffer layer exhibits a strong piezoelectric polarization. The estimated built-in electric field (parallel to the c -axis) due to the piezoelectric polarization is -0.96 MV cm^{-1} (-0.33 MV cm^{-1}) in the QW and is 0.62 MV cm^{-1} (0.30 MV cm^{-1}) in the barrier for sample 1 (sample 2) as calculated using a method developed by Fiorentini et al. [18].

3. Steady state differential transmission

Initially, we performed steady state pump/probe differential transmission measurements on these samples by pumping with a continuous-wave (CW) Ar^+ laser (3.41 eV) and probing with a Xenon lamp. The white light from the Xenon lamp was spectrally filtered using a spectrometer and

then focused to a 1 mm diameter spot on the sample to serve as the probe beam. The pump spot size was chosen to be 2 mm to ensure that the probe beam was monitoring a relatively constant injected carrier density. Standard lock-in techniques were used to measure the difference in the probe transmission (ΔT) with and without the pump present as a function of probe wavelength. The differential absorption spectrum was then extracted from differential transmission: $\Delta\alpha = -1/d[\ln(1 + \Delta T/T)]$, where d is the combined thickness of the InGaN QWs [16]. Fig. 1(a) shows the expected absorption with the pump off (solid line) and the pump on (long dashed line) for excitonic blue shifting due to field screening. The absorption with the pump on is expected to narrow and shift as a result of a reduction of the in-well field by in-well carrier screening. Fig. 1(a) also shows the expected resulting differential absorption signature (short dashed line). Fig. 1(b) shows the room temperature steady state change in absorption coefficient, $\Delta\alpha$, as a function of photon energy under a CW pump irradiance of 0.4 W cm^{-2} for both samples. The observed $\Delta\alpha$ is consistent with the expected change in absorption shown in Fig. 1(a) and is

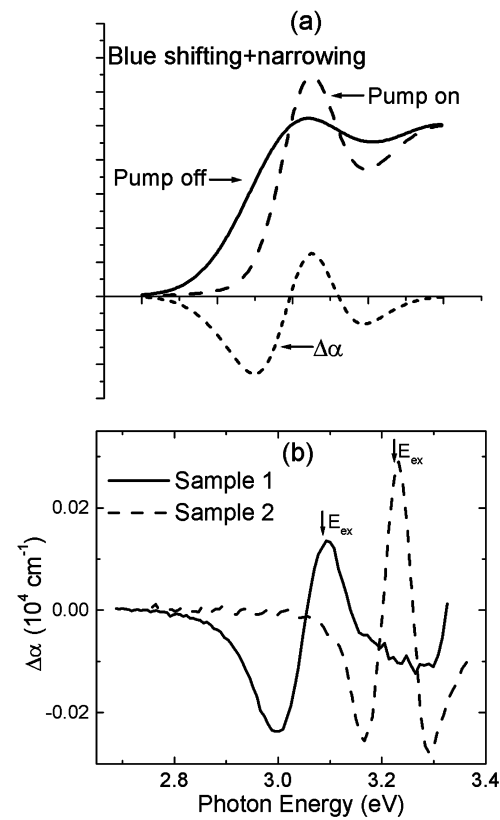


Fig. 1. (a) Schematic illustration of the expected change in absorption (short dashed line) due to field screening and narrowing of the excitonic resonance. (b) Steady state differential absorption spectra of sample 1 (solid line) and sample 2 (dashed line) at room temperature under a pump irradiance of 0.4 W cm^{-2} . The arrow indicates the excitonic resonance energy.

similar to a recent result from AlGaIn/GaN QW with a negative–positive–negative swing due to blue shifting and narrowing of the excitonic absorption [19]. In this case, when the magnitude of the internal in-well field is reduced under optical excitation, the absorption coefficient at the excitonic resonance becomes larger because of an increase of its oscillator strength and narrows in energy because of a prolongation of the excitonic lifetime. Therefore, the excitonic resonance can be estimated to be approximately at the energy of the positive peak of the change in absorption as identified in Fig. 1(b).

Of course, in Fig. 1(a) we have neglected excitonic bleaching which induces a decrease and broadening of the excitonic absorption and the corresponding change in absorption that is dominated by a large negative peak centered at the excitonic peak energy [8]. In fact, under the CW excitation intensities, we observed little evidence of excitonic bleaching and the resulting differential absorption spectra are completely consistent with field screening. The observation of the screening signature implies that under CW excitation relatively low photoinduced carrier densities are present (far below that needed to completely screen the in-well field and allow for significant bleaching to take place).

4. Time-resolved measurements

In order to confirm the insignificant carrier accumulation and to investigate the carrier transport and recombination dynamics, time-resolved PL and time-resolved differential transmission were conducted for these samples. For the time-resolved PL measurements, the 760 nm, 150 fs laser pulses from a 250 kHz regenerative amplifier (REGA) were frequency doubled to 380 nm to serve as the pump source for carrier excitation above the InGaIn bandgap, but below the GaN bandgap. Fig. 2 shows the room temperature time-resolved PL measurement on sample 1 for an excitation fluence of $400 \mu\text{J cm}^{-2}$ corresponding to a maximum two-dimensional (2D) photoexcited carrier density for each well of $7.2 \times 10^{13} \text{ cm}^{-2}$. This sheet charge carrier density is much larger than the sheet charge carrier density of $4.8 \times 10^{12} \text{ cm}^{-2}$ needed to screen the estimated in-well field. Notice that there is no observable shift of peak energy in the PL spectra versus time, and more importantly, that the peak emission energy (3.02 eV) is lower than the exciton resonance energy (3.08 eV) identified in Fig. 1. This behavior suggests that the radiative recombination in this sample is from localized states below the exciton resonance energy. Similar signatures were also observed in sample 2.

Subsequent to these time-resolved PL measurements, time-resolved differential transmission was used to determine the presence of any excess carriers that are not detected using time-resolved PL. Specifically, ultrafast single-color pump-white light continuum probe spec-

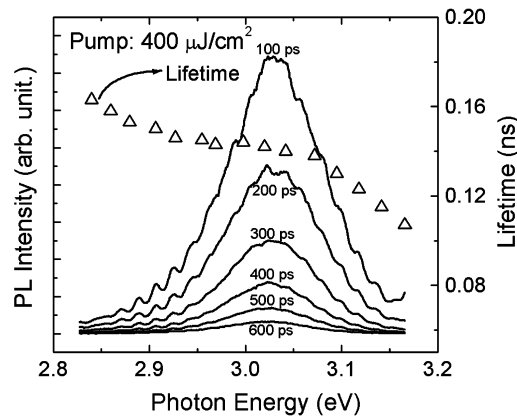


Fig. 2. Time-resolved PL spectra for sample 1 at different time delays and the corresponding photon energy dependent lifetime (triangles) at room temperature.

troscopy was used to time resolve the differential transmission signatures at room temperature. For these measurements, a portion of the 760 nm laser pulses from the REGA was frequency doubled to 380 nm to serve as the pump source. The remaining output from the REGA was used to create a broadband white light continuum [20], with spectral components from 385 to 1000 nm (1.24 to 3.22 eV), which served as the probe beam. The time delay of the probe beam with respect to the pump beam was tuned by controlling the position of a retroreflector mounted on a motor-controlled delay stage with resolution of 1.6 μm . The time resolution of this system was limited to ~ 300 fs due to the broadened pulse width of the frequency-doubled pulse and the white-light continuum. In this case, the probe beam was focused to an 80 μm diameter spot on the sample and the transmitted light was spectrally resolved using a spectrometer. The pump spot size was chosen to be 160 μm .

Fig. 3 shows the detailed differential absorption spectra under various pump fluences on sample 1 at a time delay of 40 ps. At high pump fluence the in-well field is totally screened and a single negative peak due to excitonic bleaching dominates the spectra (Fig. 3(a)). By contrast, at low pump fluence the observed spectral signature is consistent with the combination of excitonic bleaching (negative peak), and excitonic blue shifting and narrowing (undulation shown in Fig. 3(d)).

Furthermore, by temporally resolving these differential absorption spectra the different carrier decay behaviors were demonstrated. Fig. 4(a) shows the differential absorption spectra under high pump fluence ($400 \mu\text{J cm}^{-2}$) versus time delay from 2 to 400 ps for sample 1. It should be noted that with increasing time delay the peak energy exhibits a red shift but the spectra are still dominated by a single negative peak. This large negative peak is a clear indication that we still have sufficient carriers to completely screen the in-well field. The inset graph in Fig. 4(a) shows the time evolution for energy position at 3.08 eV. The observed decay time of

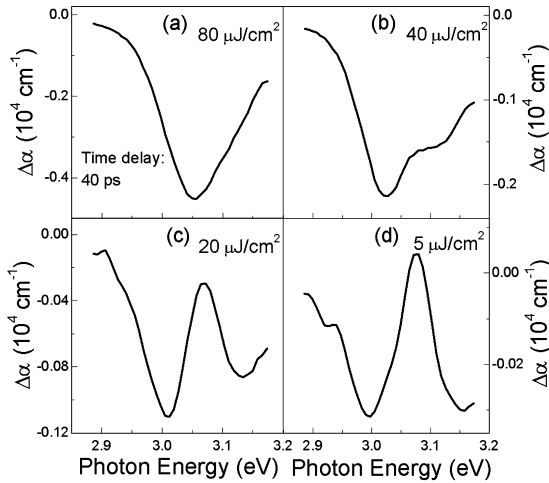


Fig. 3. Differential absorption spectra at a time delay of 40 ps for sample 1 under pump fluences of (a) $80 \mu\text{J cm}^{-2}$, (b) $40 \mu\text{J cm}^{-2}$, (c) $20 \mu\text{J cm}^{-2}$, and (d) $5 \mu\text{J cm}^{-2}$.

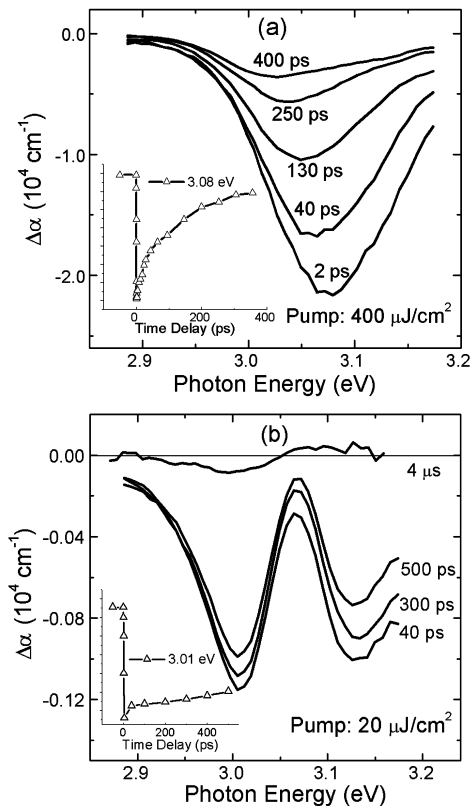


Fig. 4. (a) Differential absorption spectra at different time delays under high pump fluence ($400 \mu\text{J cm}^{-2}$) for sample 1. The inset shows the time evolution of $\Delta\alpha$ at 3.08 eV. (b) Differential absorption spectra at different time delays under low pump fluence ($20 \mu\text{J cm}^{-2}$) for sample 1. The inset shows the time evolution of $\Delta\alpha$ at 3.01 eV.

0.16 ns is consistent with the recombination lifetime determined by time-resolved PL.

In contrast, Fig. 4(b) shows the differential absorption spectra versus time delay from 40 ps to 4 μs for a pump fluence of $20 \mu\text{J cm}^{-2}$ on sample 1. (The measurement at 4 μs was made by setting the delay so that the probe pulse arrived at the sample 40 ps before the next pump pulse.) The time evolution for energy position at 3.01 eV is also shown in the inset graph in Fig. 4(b). Clearly, although the net change in absorption decreases with time delay as the carrier density decreases, the change in absorption due to screening of the in-well field remains relatively unchanged for short times. Moreover, the positive and negative peaks indicative of a field-induced excitonic blue shifting and narrowing are still evident after 4 μs . This extreme prolongation of recombination lifetime in the well is induced by the spatial separation between electrons and holes under the influence of the in-well field [8].

5. Discussion

By attributing the observed reduction in excitonic amplitude to bleaching and the observed blue shift to in-well screening, the time-resolved differential absorption spectra for sample 1 can be separated into two components, as shown in Fig. 5(a). The bleaching component was chosen from the differential absorption bleaching spectra (short time curve in Fig. 4(a)) at high pump fluence, where the peak energy of the bleaching component was 3.08 eV, corresponding to the exciton resonance. The amplitude of this signal was scaled proportionally to the pump fluence. The in-well field screening component was then obtained by subtracting the bleaching component from the original spectra. The peak absorption changes corresponding to screening, $\Delta P_{\text{screening}}$, and bleaching, $\Delta P_{\text{bleaching}}$, as shown in Fig. 5(a), were used to estimate the strength of the Stark shift induced by field screening and the strength of the absorption bleaching in the InGaN QW, respectively. The peak absorption changes caused by these two components, as estimated by the fitting, as a function of 2D photoexcited carrier density in each well are also shown separately in Fig. 5(b). As should be expected, when increasing the carrier density, the screening component approaches a constant value while the bleaching component increases linearly.

Clearly, estimating the in-well field from the observed changes in absorption is complicated. However, it is well known that as flat-band conditions are approached there is substantial envelope function overlap between the electrons and holes in the well and the $\Delta\alpha$ spectra should be indicative of excitonic bleaching and excitonic field screening. Thus, the transition point, $5.6 \times 10^{12} \text{ cm}^{-2}$, at which the bleaching and screening signatures are comparable, is a reasonable choice for estimating the in-well field (i.e. the in-well field is being sufficiently screened that the overlap of the carriers

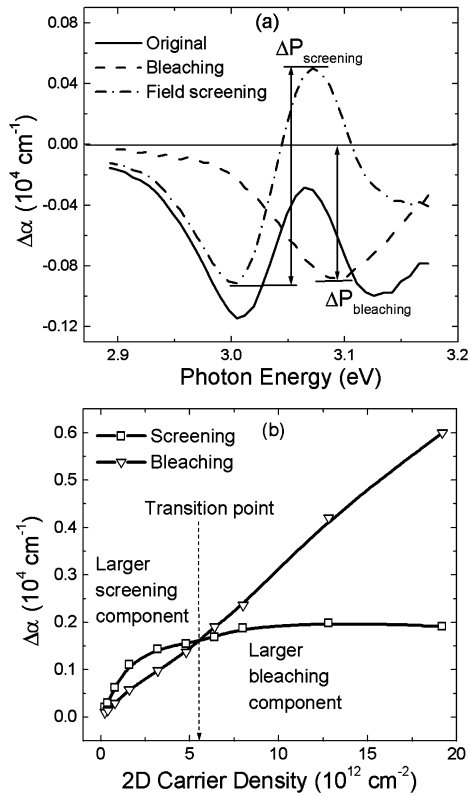


Fig. 5. (a) The differential absorption spectrum (solid line) at a time delay of 40 ps and a pump fluence of $20 \mu\text{J cm}^{-2}$ for sample 1 is separated into in-well field screening (dash dot line) and bleaching (dashed line) components. (b) The extracted peak absorption changes $\Delta P_{\text{screening}}$ and $\Delta P_{\text{bleaching}}$ versus 2D photoexcited carrier density in each well for sample 1 at the fixed time delay of 40 ps.

increases and the bleaching signature becomes significant). At this carrier density, the corresponding in-well field, 1.12 MV cm^{-1} , is close to the estimated theoretical value of 0.96 MV cm^{-1} for sample 1 provided earlier. It is important to realize that this is not an extremely accurate estimate but should provide ballpark values of the in-well field.

The experimental results presented here, illustrating excitonic bleaching and in-well field screening in these undoped InGaN/GaN MQWs, may be explained as follows. Initially, the femtosecond pulse generates excitons that are rapidly dissociated by the in-well field in the 10 nm InGaN well. At low carrier densities, the electrons and holes drift to the opposite sides of the well under the influence of the in-well field on a very fast time scale ($< 1 \text{ ps}$). Thus, the intrinsic in-well field is reduced and band bending within the well is reduced. As a result of the reduction of the magnitude of the in-well field, the differential transmission signature for excitonic blue shifting and narrowing is observed (in conjunction with excitonic bleaching). At high carrier densities, the in-well field is completely screened and the remaining carriers will fill any localized states, which

dominate the radiative recombination in these structures. Moreover, at sufficiently high carrier densities the excitonic absorption bleaching obscures the signature caused by the excitonic blue shift.

6. Conclusions

In summary, in this article a detailed study including steady state and time-resolved techniques is used to provide insight into the carrier dynamics in InGaN QWs. Specifically, we have presented carrier radiative recombination, non-radiative recombination and evidence of dominant emission below the excitonic transition corresponding to the localized states. Furthermore, measurement of the differential transmission spectra versus carrier density provides a method to separate the field screening behavior from the band-filling effects by observing the transition from the signature of excitonic absorption bleaching to excitonic blue shifting. The estimated in-well field at the transition point between the two signatures is consistent with the calculated value resulting from piezoelectric polarization in strained InGaN wells.

Acknowledgements

This work was supported by the National Science Foundation CAREER Award, NSF #9733720, under the direction of Dr Filbert Bartoli, and the Office of Naval Research Young Investigator Program Award #N00014-00-1-0508 under the direction of Dr Colin Wood.

References

- [1] S.C. Jain, M. Willander, J. Narayan, R.V. Overstraeten, *J. Appl. Phys.* 87 (2000) 965.
- [2] S. Nakamura, M. Senoh, S. Nagahama, N. Iwasa, T. Yamada, T. Matsushita, H. Kiyoku, Y. Sugimoto, T. Kozaki, H. Umemoto, M. Sano, K. Chocho, *Jpn. J. Appl. Phys. Part 2* 36 (1997) L1568.
- [3] K.P. O'Donnell, R.W. Martin, P.G. Middleton, *Phys. Rev. Lett.* 82 (1999) 237.
- [4] S. Chichibu, K. Wada, S. Nakamura, *Appl. Phys. Lett.* 71 (1997) 2346.
- [5] T. Takeuchi, S. Sota, M. Katsuragawa, M. Komori, H. Takeuchi, H. Amano, I. Akasaki, *Jpn. J. Appl. Phys. Part 2* 36 (1997) L382.
- [6] X.R. Huang, A.N. Cartwright, D.R. Harken, D.S. McCallum, A.L. Smirl, J.L. Sánchez-Rojas, A. Sacedón, E. Calleja, E. Muñoz, *J. Appl. Phys.* 79 (1995) 417.
- [7] X.R. Huang, D.R. Harken, A.N. Cartwright, A.L. Smirl, J.L. Sánchez-Rojas, A. Sacedón, E. Calleja, E. Muñoz, *Appl. Phys. Lett.* 67 (1995) 950.
- [8] A.N. Cartwright, D.S. McCallum, T.F. Boggles, A.L. Smirl,

- T.S. Moise, L.J. Guido, R.C. Barker, B.S. Wherrett, *J. Appl. Phys.* 73 (1993) 7767.
- [9] T. Kuroda, A. Tackeuchi, *J. Appl. Phys.* 92 (2002) 3071.
- [10] P. Riblet, H. Hirayama, A. Kinoshita, A. Hirata, T. Sugano, Y. Aoyagi, *Appl. Phys. Lett.* 75 (1999) 2241.
- [11] P.G. Eliseev, P. Perlin, J. Lee, M. Osiński, *Appl. Phys. Lett.* 71 (1997) 569.
- [12] S. Chichibu, T. Azuhata, T. Sota, S. Nakamura, *Appl. Phys. Lett.* 70 (1997) 2822.
- [13] S. Chichibu, T. Sota, K. Wada, S. Nakamura, *J. Vac. Sci. Technol. B* 16 (1998) 2204.
- [14] E. Kuokstis, J.W. Yang, G. Simin, M.A. Khan, R. Gaska, M.S. Shur, *Appl. Phys. Lett.* 80 (2002) 977.
- [15] A. Satake, Y. Masumoto, T. Miyajima, T. Asatsuma, M. Ikeda, *Phys. Rev. B* 60 (1999) 16660.
- [16] Y. Kawakami, Y. Narukawa, K. Omae, S. Nakamura, S. Fujita, *Mater. Sci. Engng B* 82 (2001) 188.
- [17] Ü. Özgür, M.J. Bergmann, H.C. Casey, H.O. Everitt, A.C. Abare, S. Keller, S.P. Denbaars, *Appl. Phys. Lett.* 77 (2000) 109.
- [18] V. Fiorentini, F. Bernardini, F.D. Sala, A.D. Carlo, P. Lugli, *Phys. Rev. B* 60 (1999) 8849.
- [19] A. Shikanai, T. Deguchi, T. Sota, T. Kuroda, A. Tackeuchi, S. Chichibu, S. Nakamura, *Appl. Phys. Lett.* 76 (2000) 454.
- [20] C. Nagura, A. Suda, H. Kawano, M. Obara, K. Midorikawa, *Appl. Opt.* 41 (2002) 3735.